Matter and Radiation at Extremes | RESEARCH ARTICLE | scitation.org/journal/mre

High-energy-density metal nitrides with armchair chains

Cite as: Matter Radiat. Extremes 7, 038402 (2022); doi: 10.1063/5.0087168
Submitted: 2 February 2022 • Accepted: 14 March 2022 •
Published Online: 8 April 2022

Jianan Yuan,[1] Kang Xia,[2] Chi Ding,[1] Xiaomeng Wang,[1] Qing Lu,[1] and Jian Sun[1,a)]

AFFILIATIONS

[1]National Laboratory of Solid State Microstructures, School of Physics and Collaborative Innovation Center of Advanced Microstructures, Nanjing University, Nanjing 210093, People's Republic of China
[2]Department of Applied Physics, College of Science, Nanjing Forestry University, Nanjing 210037, China

[a)]**Author to whom correspondence should be addressed:** jiansun@nju.edu.cn

ABSTRACT

Polymeric nitrogen has attracted much attention owing to its possible application as an environmentally safe high-energy-density material. Based on a crystal structure search method accelerated by the use of machine learning and graph theory and on first-principles calculations, we predict a series of metal nitrides with chain-like polynitrogen ($P2_1$-AlN_6, $P2_1$-GaN_6, P-1-YN_6, and $P4/mnc$-TiN_8), all of which are estimated to be energetically stable below 40.8 GPa. Phonon calculations and *ab initio* molecular dynamics simulations at finite temperature suggest that these nitrides are dynamically stable. We find that the nitrogen in these metal nitrides can polymerize into two types of poly-N_4^{2-} chains, in which the π electrons are either extended or localized. Owing to the presence of the polymerized N_4 chains, these metal nitrides can store a large amount of chemical energy, which is estimated to range from 4.50 to 2.71 kJ/g. Moreover, these compounds have high detonation pressures and detonation velocities, exceeding those of conventional explosives such as TNT and HMX.

I. INTRODUCTION

Molecular nitrogen (N_2) is the most abundant component of Earth's atmosphere and one of the most stable molecules owing to its strong N≡N triple bond. There is a large energy difference between single/double nitrogen bonds (160 and 418 kJ/mol for N–N and N=N, respectively) and the N≡N triple bond (954 kJ/mol).[1] Therefore, polynitrogen composed of mixed single and double bonds can store a substantial amount of chemical energy. The stored energy will be released when decomposition of the polymeric nitrogen is triggered, producing pollution-free N_2 molecules, in an oxygen-free process. However, the high bond energy of the N_2 molecule makes it highly unreactive. It is difficult to synthesize polymeric nitrogen from N_2 molecules. To break nitrogen triple bonds and obtain nitrogen polymers, extreme conditions such as high pressures and high temperatures become necessary to overcome the high energy barriers.[2,3] For example, pressure can be used to break the nitrogen bonds, with the formation of some unexpected nitrogen compounds.[4] In some nitrogen-rich cases, pressure can enhance the effect of electronic delocalization, thus helping to dissociate molecules and form polymeric structures.

Tremendous efforts have been made to obtain novel polymeric nitrogen structures under high pressures in both theoretical and experimental studies.[2,3,5–9] More than a decade after its theoretical prediction by Mailhiot *et al.*,[5] an experimental breakthrough was eventually made by Eremets *et al.* in 2004 in their synthesis of a cubic-gauche nitrogen structure (cg-N).[2] This cg-N contains pure N–N single bonds and thus possesses an extremely high energy density, which is reported to be five times higher than that of the current most powerful energetic materials.[5] Since then, several polymeric nitrogen structures have been synthesized: hexagonal layered polymeric nitrogen (HLP-N), layered polymeric nitrogen (LP-N), and a black phosphorus structure (BP-N).[10–13] However, the pressure–temperature conditions required for these polymeric nitrogen syntheses are very high, exceeding 110 GPa and 2000 K. Such extreme conditions cause great practical difficulties, and therefore the search for potential high-energy-density materials (HEDMs) that can be synthesized under moderate pressures is still an important task.

Recently, counter-ions and nitrogen fragments have been used to construct nitrogen-bearing compounds involving ionic bonding, including N_5 and N_6 rings, nitrogen azide, and polymeric N_4 chains (poly-N_4^{2-}).[7,14–28] In these cases, the ionic bonds can enhance the

kinetic stability of the polynitride components and reduce the pressure required for synthesis. Among these nitrogen fragments, poly-N_4^{2-} has become of particular importance. Previous theoretical works have predicted the existence of several poly-N_4^{2-} compounds, including BeN_4, MgN_4, CaN_4, CdN_4, and FeN_4.[29–33] Of these, MgN_4, FeN_4, TaN_4, and BeN_4 have recently been synthesized.[34–37] Typical alkaline-earth nitrides such as the BeN_4, MgN_4, and CaN_4 compounds,[29,30,32] have similar N–N bond lengths in the range 1.32–1.35 Å. However, the poly-N_4^{2-} chains in FeN_4[34] possess significantly different N–N bond lengths, between 1.29 and 1.43 Å. Nevertheless, these poly-N_4^{2-} chains are constructed with N–N single bonds and N=N double bonds, matching the features of HEDM nitrides. Additionally, the N_2^- species is found to coexist with the poly-N_4^{2-} chain in some high-energy-density metal nitrides synthesized by Bykov *et al.*[38,39] The cations in these structures are mainly divalent metals. We envision that the nitrogen content of metal nitrides can be increased by the use of metal ions in higher valence states, thereby achieving higher energy densities.

In this work, we focus on the metals Al, Ga, Y and Ti, which can provide three or four valence electrons. We predict that the poly-N_4^{2-} chain can occur in four new metal nitride crystals MN_x with different symmetries: $P2_1$-AlN_6, $P2_1$-GaN_6, P-1-YN_6, and $P4/mnc$-TiN_8. These are predicted to be energetically stable at moderate pressures. Molecular dynamics (MD) simulations and phonon spectrum calculations suggest that these MN_x are mechanically stable at nonzero temperatures and high pressures. More interestingly, we find coexistence of the aforementioned two types of poly-N_4^{2-} chains, appearing in our predicted $P2_1$ phase of the AlN_6 and GaN_6 compounds. Besides, we estimate that these MN_x have excellent detonation properties and can served as potential HEDMs.

II. METHODS

We carry out a crystal structure search using MAGUS ("machine learning and graph theory assisted universal structure searcher"),[40,41] which is accelerated through the use of graph theory[42] and machine learning potentials. This method has been successfully applied to many systems.[40,43–48] To generate new structures containing the desired N_4^{2-} units, molecular-based unit searches are conducted at 50 GPa. We constrain four MN_x formula units into one cell to explore more nitrogen-containing configurations. The first-principles calculations are performed using the Vienna *Ab initio* Simulation Package (VASP).[49] Density-functional theory (DFT) is implemented within the projector-augmented-wave (PAW) approach.[50] We use the Perdew–Burke–Erzernhof functional based on the generalized gradient approximation[51,52] to describe the exchange–correlation interaction. Van der Waals (vdW) effects are taken into account using the DFT-D3 method in VASP.[53,54] The valence electrons occupying the shell states are $3s^23p^1$, $4s^24p^1$, $4s^24p^65s^14d^2$, and $3p^64s^23d^2$ for Al, Ga, Y, and Ti, respectively. The energy cutoff of the plane-wave basis is set at 1050 eV. The Brillouin zone is separated with k-meshes of $2\pi \times 0.03$ Å^{-1} to guarantee convergence of energy. We use the PHONOPY code[55] to calculate the phonon spectrum for a $2 \times 2 \times 2$ supercell. Projected crystal orbital Hamilton population (pCOHP) calculations are conducted using the LOBSTER code.[56,57] Noncovalent interactions are also taken into consideration by calculating the reduced density gradient (RDG) using the Critic2 code.[58,59] The structures are visualized by VESTA software.[60] We analyze the electronic properties in the context of molecular orbital (MO) theory.[61]

III. RESULTS AND DISCUSSION

Using the crystal structure search method described above, we predict several metal nitrides structures, as shown in Figs. 1(a)–1(c). Diverse channel frames are constructed from different coordinate bonds between metal atoms and poly-N_4^{2-} chains [Figs. 1(d)–1(f)]. These channel-like structures may capture small molecules, such as N_2 or H_2O, all of which stabilize these metal nitrides.[17,18,39] For AlN_6 and GaN_6 in the $P2_1$ phase, one metal atom is found to be coordinated with three or four chains of poly-N_4^{2-} [Fig. 1(d)]. As shown in Fig. 1(e), one metal atom in the P-1-YN_6 structure is sevenfold-coordinated with nitrogen atoms. Because N_2 double balls coexist with poly-N_4^{2-} chains in the P-1-YN_6 structure, we can describe the YN_6 within a unit cell as $Y_4(N_2)_2(N_4)_5$. For $P4/mnc$-TiN_8, the poly-N_4^{2-} chain is fourfold-coordinated around one Ti atom [Fig. 1(f)].

We calculate the relative enthalpy of MN_x (M = Al, Ga, Y, and Ti) as shown in Fig. 2. By taking the enthalpy difference of MN_x relative to the ground-state metal nitrides (MN) plus bulk nitrogen phase at these pressures, $\Delta H = MN_x - MN - (x-1)N$, we can confirm the energetic stabilities of MN_x compounds under pressure. Here, the Pa-3 (α) and $P4_12_12$ phases of the N_2 molecular crystal structures are selected for the relative-enthalpy calculations at 0 GPa and at higher pressures, respectively.[65] Fm-3m-MN is chosen as the ground state for the Al–N, Y–N and Ti–N systems. The ground state for the GaN structure in the Ga–N system favors the $P6_3/mmc$ phase, which tends to transform into the Fm-3m phase above 32.5 GPa.[62] We find that AlN_6, GaN_6, and TiN_8 are enthalpically stable above pressures of around 40.8, 39.3, and 40.1 GPa, respectively. However, YN_6 turns out to be stable above a much lower external pressure (around 21.7 GPa). Therefore, we suggest that MN_x might be synthesized at moderate pressures around 40 GPa or lower. In addition, no imaginary frequency of the phonon spectrum has been found in the Brillouin zones of these MN_x structures, indicating their dynamical stability, as shown in Fig. S1 in the supplementary material. Among them, in particular, $P4/mnc$-TiN_8 is quenchable to 0 GPa.

To confirm the thermal stabilities of the newly predicted MN_x, we conduct *ab initio* molecular dynamics (AIMD) simulations for the MN_x ($2 \times 2 \times 2$) supercells at high temperatures for 12 ps with an interval of 1 fs. The supercells contain 224 atoms for the AlN_6, GaN_6, and YN_6 structures and 144 atoms for TiN_8. The AIMD calculations are performed within the canonical ensemble for AlN_6 and GaN_6 at 20 GPa, for YN_6 at 40 GPa, and for TiN_8 at 30 GPa. The resulting radial distribution functions (RDFs) are presented in Fig. 3 and in Fig. S2 in the supplementary material. The sharp peak around 1.30 Å in Fig. 3 represents the N–N bonds within N_4 units in the balanced structures. It matches well with the N–N bond length in the original structures (the vertical dashed line). Therefore, the N_4 units remain intact to at least 1200 K for AlN_6, GaN_6, and TiN_8, and 900 K for YN_6. The insets show the stable averaged structures at the corresponding temperatures. In addition, the RDFs of metal–nitrogen (M–N) pairs and metal–metal (M–M) pairs (Fig. S2 in the supplementary material) suggest that the M–N and M–M pairs remain stable up to the corresponding temperatures. At higher temperatures, the MN_x frameworks begin to decompose. We use the mean-squared displacement (MSD), which represents the overall particle deviation, to measure

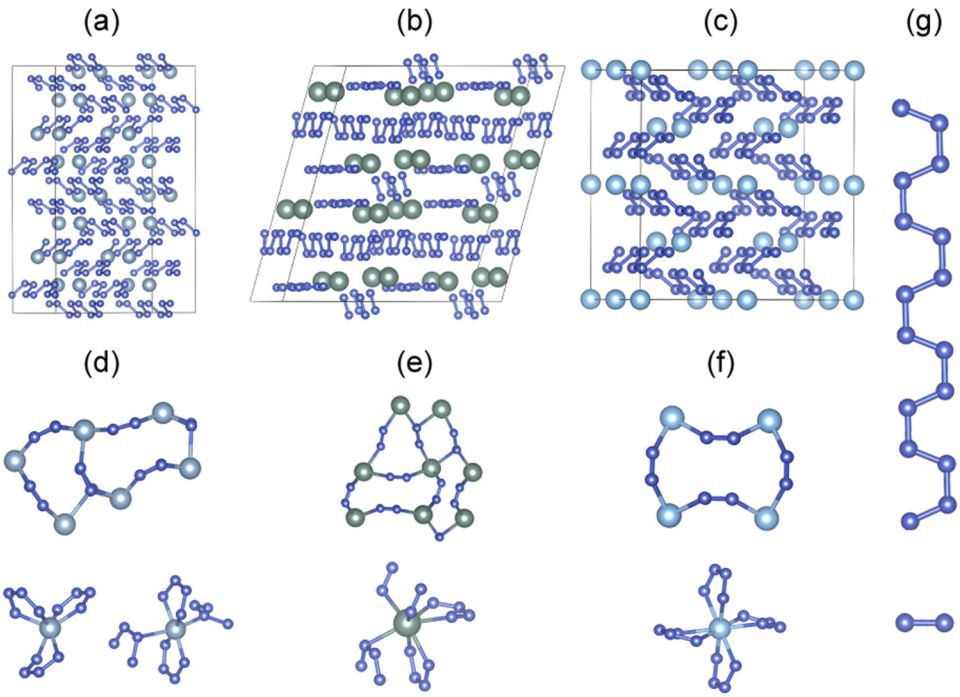

FIG. 1. (a) Isostructural AlN_6 and GaN_6 of the $P2_1$ phase at 20 GPa. (b) and (c) Crystal structures of P-1-YN_6 at 40 GPa and $P4/mnc$-TiN_8 at 30 GPa, respectively. (d)–(f) geometries of channels formed by metal atoms with different types of N_4 coordination. (g) Typical poly-N_4^{2-} chain and nitrogen dimer N_2.

whether the MN_x break down. The MSD function is defined by $MSD(t) = u\langle|r_i(t) - r_i(0)|^2\rangle$, where $r_i(t)$ and $r_i(0)$ are the positions of atom i at time t and the initial time, respectively. Figure S3 in the supplementary material presents the MSDs for AlN_6 at 3000 K, GaN_6 at 2500 K, YN_6 at 1200 K, and TiN_8 at 2500 K. The increases in MSDs mean that the MN_x exhibit diffusive tendencies. Also, as shown by Fig. S4 in the supplementary material, the structures of MN_x at 12 ps exhibit large deviations from the original structures. Some N–N bonds in poly-N_4^{2-} chains are stretched or broken. Depending on the degree of decomposition, the poly-N_4^{2-} chains become separate N_4, N_3, or N_2 units, and so we can deduce that MN_x will break down at the corresponding temperatures.

The calculated density of states (DOS) exhibits metallic features for all MN_x structures, as shown in Figs. 4(a)–4(d). The main

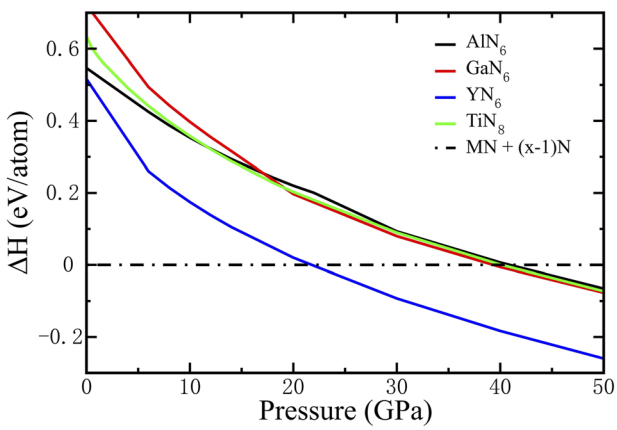

FIG. 2. Enthalpy difference of MN_x (M = Al, Ga, Y, and Ti) relative to that of a mixture of ground-state MN (M = Al, Ga, Y, and Ti)[24,62–64] structure and bulk nitrogen phase.[65]

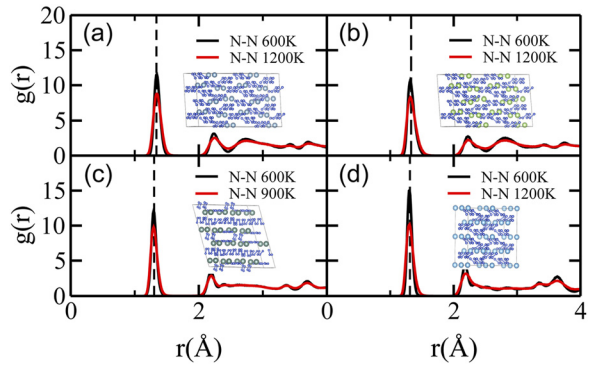

FIG. 3. (a)–(d) Radial distribution functions (RDFs) $g(r)$ for MN_x structures from MD simulations. The nitrogen-to-nitrogen pair (N–N) RDFs at different temperatures are shown as solid lines for (a) $P2_1$-AlN_6, (b) $P2_1$-GaN_6, (c) P-1-YN_6, and (d) $P4/mnc$-TiN_8. Vertical dashed lines represent the averaged distance between nitrogen atoms in the structures relaxed at 0 K. The inset graphics show the corresponding statistically averaged structures.

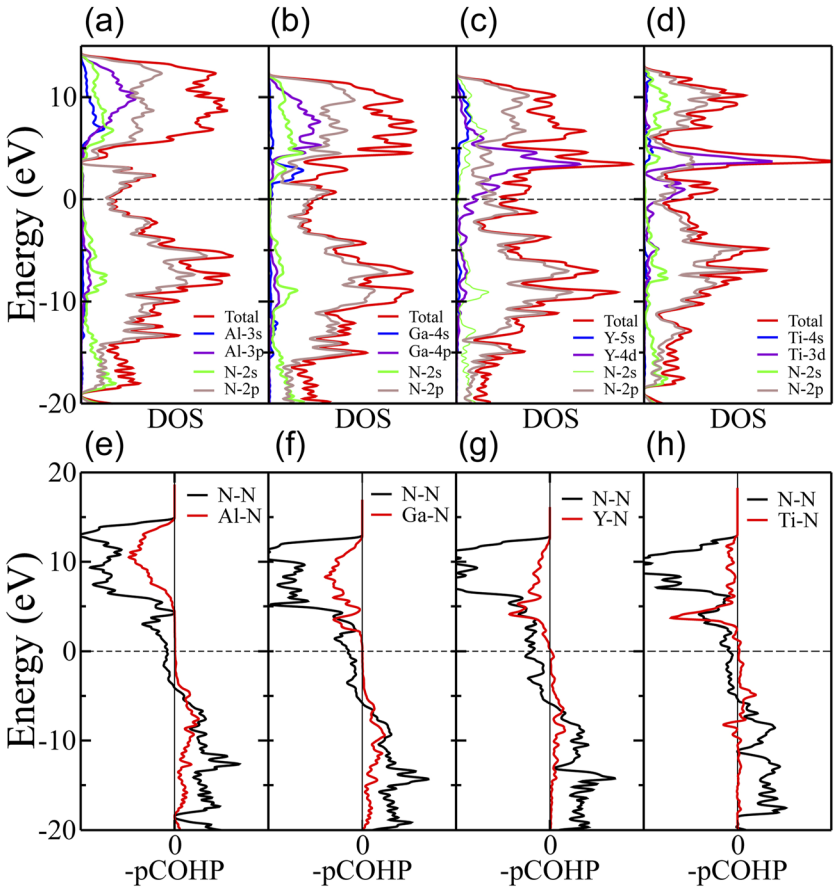

FIG. 4. (a)–(d) Density of states (DOS) and (e)–(h) minus projected crystal orbital Hamilton population (−pCOHP) for $P2_1$-AlN_6 [(a) and (e)], $P2_1$-GaN_6 [(b) and (f)], P-1-YN_6 [(c) and (g)], and $P4/mnc$-TiN_8 [(d) and (h)]. The dashed line indicates the Fermi energy level.

contribution to the DOS at the Fermi energy is from the N-2p orbital for the AlN_6 and GaN_6 structures, while the d orbitals of the transition metals Y and Ti make additional contributions to the DOS around the Fermi energy for YN_6, and TiN_8. We carry out a projected crystal orbital Hamilton population (pCOHP) calculation to distinguish the bond features in the predicted MN_x nitrides. Using minus pCOHP (−pCOHP), we can partition the bond energy into bonding states with positive values and antibonding states with negative values. Figures 4(e)–4(h) reveal similar bond features for these four structures. For N–N bonds, although most of the states below the Fermi level can be attributed to bonding states, there are still some antibonding states existing just below the Fermi level. For M–N bonds, however, almost all the states below the Fermi level are bonding states. The minus integral pCOHP (−IpCOHP)[66] values at the Fermi level, which represent the pairwise interatomic interaction strength, are listed in Table I. The −IpCOHP values of N–N bonds are at least twice those of M–N bonds, which suggests that the N–N bonds have greater pairwise interatomic interaction strengths than the M–N bonds.

To explain the electronic features of MN_x, we apply MO theory[61] to analyze the electron orbitals and describe the coordination of the metal atoms. For the isostructural AlN_6 and GaN_6, two types of poly-N_4^{2-} chains (types A and B) are sketched in Figs. 5(a) and 5(b), respectively. Each N atom in type A [Fig. 5(a)] is surrounded by three atoms in a nearly planar triangular geometry, suggesting sp^2 hybridization. Of a total of 22 electrons in one N_4^{2-} unit, 16 are found to occupy eight sp^2 hybrid orbitals. The extra four p orbitals of four nitrogen atoms form four π orbitals. The remaining electrons occupying π orbitals form delocalized π bonds, which is the origin of metallicity. The equally distributed π band also explains why the N–N bond lengths (1.32–1.33 Å) are between those of an N–N single bond

TABLE I. Average −IpCOHP values for MN_x.

Compound	Average −IpCOHP/bonds (eV/bond)	
	M–N	N–N
$P2_1$-AlN_6	4.83	14.26
$P2_1$-GaN_6	4.28	14.51
P-1-YN_6	3.12	15.30
$P4/mnc$-TiN_8	2.72	12.46

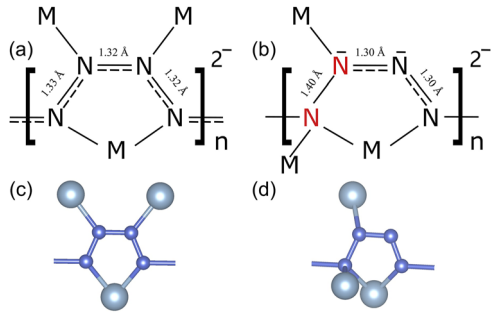

FIG. 5. Sketches of (a) type A and (b) type B chains for N_4–metal coordination, and fragment structures of (c) type A and (d) type B poly-N_4^{2-} chains.

(1.45 Å) and an N=N double bond (1.20 Å).[29] As shown in Fig. 5(b), for the type B poly-N_4^{2-} chain, the two N atoms colored red possess tetrahedral coordination including lone pairs, indicating their sp^3 hybridization, while the other two N atoms are sp^2-hybridized, similar to those in Fig. 5(a), and therefore the extra two p atomic orbitals of these two N atoms form one bonding orbital π and one antibonding orbital π^*. The remaining two electrons occupying the bonding π orbital form a π bond, distributed over the sp^2-hybridized N atoms. This can explain why the length of the bond between the two sp^3-hybridized N atoms is 1.40 Å, which is close to that of an N–N single bond (1.45 Å), but the length of the bond connecting the sp^2-hybridized N atoms is 1.30 Å, which is between those of single and double bonds. Therefore, the N–N bonds in the type A chain are all hybridized bonds, while those in the type B chain are half-single, half-hybridized. In terms of bond energy, the type B chain may possess a higher energy capability in principle. However, YN_6 and TiN_8 contain only type A poly-N_4^{2-} chains.

When the electron density ρ is too low to allow analysis of the results for the electron localization function, we can identify the noncovalent interactions (NCIs) by calculating the reduced density gradient (RDG) s, which is defined as

$$s = \frac{1}{2(3\pi^2)^{1/3}} \frac{|\nabla\rho|}{\rho^{4/3}}.$$

As shown in Fig. 6, a plot of s vs ρ multiplied by the sign of the second Hessian eigenvalue of $\nabla^2\rho$, i.e., sign(λ_2),[59,67] reveals the basic partition of the intramolecular interactions, including weak NCIs. Here, sign(λ_2) identifies the attractive weak interactions (negative, far left), repulsive weak interactions (positive, far right), and van der Waals interactions (around zero). The obvious spikes at low ρ, with much faster decrease of the gradient of ρ, indicate the existence of van der Waals interactions in the MN_x structures. To visualize these results in real space, we have plotted three-dimensional representations with an isosurface value of s = 0.5 a.u. using the VMD software[68] in Fig. S6 in the supplementary material. In this figure, green regions correspond to the van der Waals interactions between poly-N_4^{2-} chains in MN_x. In addition, we can see some blue regions around metal atoms, which correspond to the attractive interaction between metal atoms and poly-N_4^{2-} chains.

Nitrides containing poly-N_4^{2-} chains have been synthesized for potential applications as HEDMs.[34–37] This inspires us to study the detonation performance of the MN_x structures predicted in this work,

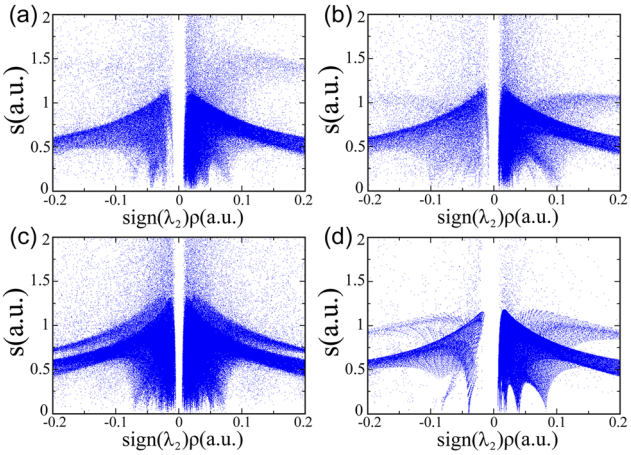

FIG. 6. Plots of the RDG s vs electron density multiplied by the sign of the second Hessian eigenvalue for (a) $P2_1$-AlN_6, (b) $P2_1$-GaN_6, (c) P-1-YN_6, and (d) $P4/mnc$-TiN_8.

TABLE II. Comparison of the detonation properties of MN_x structures estimated using the Kamlet–Jacobs empirical equations[22,69] with the corresponding experimental values for TNT and HMX.[70]

	ρ (g/cm^3)	E_g (kJ/g)	E_v (kJ/cm^3)	V (km/s)	P (kbar)
AlN_6	1.93	4.41	8.54	10.30	462
GaN_6	3.48	3.94	13.75	10.38	1020
YN_6	4.00	2.71	10.86	12.67	993
TiN_8	2.91	4.50	13.10	13.43	1024
TNT	1.64	4.30	7.05	6.90	190
HMX	1.90	5.70	10.83	9.10	393

which have more poly-N_4^{2-} chains than the previously proposed structures. We assume that MN_x will decompose into MN and N_2 gas under ambient conditions: $MN_x\,(s) \rightarrow MN\,(s) + \frac{1}{2}(x-1)N_2\,(g)$. The estimated detonation properties of MN_x are listed in Table II. In particular, the energy densities of MN_x exceed that of TNT (4.30 kJ/g), except for $P2_1$-GaN_6 and P-1-YN_6. We calculate their detonation pressures P and detonation velocities V using the Kamlet–Jacobs empirical equations[22,69] $P = 15.58\rho^2 NM^{0.5}E_g^{0.5}$ and $V = 1.01\,(NM^{0.5}E_g^{0.5})^{0.5}(1 + 1.30\rho)$, where N is the number of moles of N_2 gas generated during the decomposition of 1 g of MN_x and M is the molar mass of N_2 (28 g/mol). As can be seen from Table II, MN_x have excellent detonation pressures and detonation velocities that are higher than those of the explosives TNT and HMX.

IV. CONCLUSIONS

By applying a structure search method accelerated by machine learning, we have successfully predicted four metal nitrides constructed from poly-N_4^{2-} chains: $P2_1$-AlN_6, $P2_1$-GaN_6, P-1-YN_6, and $P4/mnc$-TiN_8. Based on first-principles calculations, we have found that the pressures required for synthesis of $P2_1$-AlN_6, $P2_1$-GaN_6, and $P4/mnc$-TiN_8 are around 40 GPa, and that required for P-1-YN_6 is near 20 GPa. Phonon calculations suggest that $P4/mnc$-TiN_8 is

mechanically stable at ambient pressure, while the other three structures are mechanically stable at high pressures. Furthermore, the dynamical stabilities of MN_x at nonzero temperature have been shown by molecular dynamics simulations. Two types of poly-N_4^{2-} chains are found: in type A, all the N atoms are sp^2-hybridized and form delocalized π bonds distributed along the entire chain; in type B, half of the nitrogen atoms are sp^3-hybridized, while the other half adopt sp^2 hybridization, and so π bonding can only occur for some of the N–N bonds in the poly-N_4^{2-} chain. The results for DOS and pCOHP also confirm the MO analysis. The metallicity of MN_x stems from the delocalized π bonds. RDG calculations reveal that the effect of NCIs also helps to stabilize these MN_x structures. Most importantly, we estimate that the newly predicted MN_x have good detonation properties with potential applications as HEDMs. Furthermore, our predictions here can provide some guidance for future experiments.

SUPPLEMENTARY MATERIAL

See the supplementary material for crystal structure data and supplementary figures.

ACKNOWLEDGMENTS

J.S. gratefully acknowledges financial support from the National Natural Science Foundation of China (Grant Nos. 12125404, 11974162, and 11834006), and the Fundamental Research Funds for the Central Universities. K.X. acknowledges support from the National Natural Science Foundation of China under Grant No. 12004185, the Natural Science Foundation of the Jiangsu Higher Education Institutions of China under Grant No. 20KJB140016, and the Scientific Research Start-up Funds of Nanjing Forestry University (No. 163101110), and financial support from a Project funded by the China Postdoctoral Science Foundation (Grant No. 2019M651767). The calculations were carried out using supercomputers at the High Performance Computing Center of the Collaborative Innovation Center of Advanced Microstructures, the High-Performance Supercomputing Center of Nanjing University, and the High-Performance Computing Facility of Nanjing Forestry University.

AUTHOR DECLARATIONS

Conflict of Interest

The authors have no conflicts to disclose.

DATA AVAILABILITY

The data supporting the findings of this study are available within the article and its supplementary materials.

REFERENCES

[1]D. P. Stevenson, "The strengths of chemical bonds," J. Am. Chem. Soc. **77**, 2350 (1955).
[2]M. I. Eremets, A. G. Gavriliuk, I. A. Trojan, D. A. Dzivenko, and R. Boehler, "Single-bonded cubic form of nitrogen," Nat. Mater. **3**, 558–563 (2004).
[3]B. A. Steele, E. Stavrou, J. C. Crowhurst, J. M. Zaug, V. B. Prakapenka, and I. I. Oleynik, "High-pressure synthesis of a pentazolate salt," Chem. Mater. **29**, 735–741 (2017).
[4]M. Miao, Y. Sun, E. Zurek, and H. Lin, "Chemistry under high pressure," Nat. Rev. Chem. **4**, 508–527 (2020).
[5]C. Mailhiot, L. H. Yang, and A. K. McMahan, "Polymeric nitrogen," Phys. Rev. B **46**, 14419–14435 (1992).
[6]A. Vij, W. W. Wilson, V. Vij, F. S. Tham, J. A. Sheehy, and K. O. Christe, "Polynitrogen chemistry. Synthesis, characterization, and crystal structure of surprisingly stable fluoroantimonate salts of N_5^+," J. Am. Chem. Soc. **123**, 6308–6313 (2001).
[7]D. Laniel, G. Weck, G. Gaiffe, G. Garbarino, and P. Loubeyre, "High-pressure synthesized lithium pentazolate compound metastable under ambient conditions," J. Phys. Chem. Lett. **9**, 1600–1604 (2018).
[8]Y. Li, X. Feng, H. Liu, J. Hao, S. A. T. Redfern, W. Lei, D. Liu, and Y. Ma, "Route to high-energy density polymeric nitrogen *t*-N via He–N compounds," Nat. Commun. **9**, 722 (2018).
[9]N. P. Salke, K. Xia, S. Fu, Y. Zhang, E. Greenberg, V. B. Prakapenka, J. Liu, J. Sun, and J. F. Lin, "Tungsten hexanitride with single-bonded armchairlike hexazine structure at high pressure," Phys. Rev. Lett. **126**, 065702 (2021).
[10]D. Tomasino, M. Kim, J. Smith, and C.-S. Yoo, "Pressure-induced symmetry-lowering transition in dense nitrogen to layered polymeric nitrogen (LP-N) with colossal Raman intensity," Phys. Rev. Lett. **113**, 205502 (2014).
[11]D. Laniel, G. Geneste, G. Weck, M. Mezouar, and P. Loubeyre, "Hexagonal layered polymeric nitrogen phase synthesized near 250 GPa," Phys. Rev. Lett. **122**, 066001 (2019).
[12]D. Laniel, B. Winkler, T. Fedotenko, A. Pakhomova, S. Chariton, V. Milman, V. Prakapenka, L. Dubrovinsky, and N. Dubrovinskaia, "High-pressure polymeric nitrogen allotrope with the black phosphorus structure," Phys. Rev. Lett. **124**, 216001 (2020).
[13]C. Ji, A. A. Adeleke, L. Yang, B. Wan, H. Gou, Y. Yao, B. Li, Y. Meng, J. S. Smith, V. B. Prakapenka, W. Liu, G. Shen, W. L. Mao, and H. K. Mao, "Nitrogen in black phosphorus structure," Sci. Adv. **6**, eaba9206 (2020).
[14]F. Peng, Y. Yao, H. Liu, and Y. Ma, "Crystalline LiN_5 predicted from first-principles as a possible high-energy material," J. Phys. Chem. Lett. **6**, 2363–2366 (2015).
[15]S. Zhu, F. Peng, H. Liu, A. Majumdar, T. Gao, and Y. Yao, "Stable calcium nitrides at ambient and high pressures," Inorg. Chem. **55**, 7550–7555 (2016).
[16]B. A. Steele and I. I. Oleynik, "Sodium pentazolate: A nitrogen rich high energy density material," Chem. Phys. Lett. **643**, 21–26 (2016).
[17]C. Zhang, C. Sun, B. Hu, C. Yu, and M. Lu, "Synthesis and characterization of the pentazolate anion *cyclo*-N_5^- in $(N_5)_6(H_3O)_3(NH_4)_4Cl$," Science **355**, 374–376 (2017).
[18]Y. Xu, Q. Wang, C. Shen, Q. Lin, P. Wang, and M. Lu, "A series of energetic metal pentazolate hydrates," Nature **549**, 78–81 (2017).
[19]P. Hou, L. Lian, Y. Cai, B. Liu, B. Wang, S. Wei, and D. Li, "Structural phase transition and bonding properties of high-pressure polymeric CaN_3," RSC Adv. **8**, 4314–4320 (2018).
[20]B. Huang and G. Frapper, "Barium–nitrogen phases under pressure: Emergence of structural diversity and nitrogen-rich compounds," Chem. Mater. **30**, 7623–7636 (2018).
[21]Z. Liu, D. Li, Y. Liu, T. Cui, F. Tian, and D. Duan, "Metallic and anti-metallic properties of strongly covalently bonded energetic AlN_5 nitrides," Phys. Chem. Chem. Phys. **21**, 12029–12035 (2019).
[22]K. Xia, X. Zheng, J. Yuan, C. Liu, H. Gao, Q. Wu, and J. Sun, "Pressure-stabilized high-energy-density alkaline-earth-metal pentazolate salts," J. Phys. Chem. C **123**, 10205–10211 (2019).
[23]K. Xia, J. Yuan, X. Zheng, C. Liu, H. Gao, Q. Wu, and J. Sun, "Predictions on high-power trivalent metal pentazolate salts," J. Phys. Chem. Lett. **10**, 6166–6173 (2019).
[24]D. Zhang, X. Xu, M. Lu, T. Bi, Y. Tian, S. Zhang, Y. Yan, Y. Du, M. Zhang, and L. Gao, "Predicted crystal structures of titanium nitrides at high pressures," Comput. Mater. Sci. **180**, 109720 (2020).
[25]X. Shi, Z. Yao, and B. Liu, "New high pressure phases of the Zn–N system," J. Phys. Chem. C **124**, 4044–4049 (2020).
[26]B. Wang, R. Larhlimi, H. Valencia, F. Guégan, and G. Frapper, "Prediction of novel tin nitride Sn_xN_y phases under pressure," J. Phys. Chem. C **124**, 8080–8093 (2020).

[27]J. Zhang, C. Niu, H. Zhang, J. Zhao, X. Wang, and Z. Zeng, "Polymerization of nitrogen in nitrogen–fluorine compounds under pressure," J. Phys. Chem. Lett. **12**, 5731–5737 (2021).
[28]J. Yuan, K. Xia, J. Wu, and J. Sun, "High-energy-density pentazolate salts: CaN_{10} and BaN_{10}," Sci. China: Phys., Mech. Astron. **64**, 218211 (2021).
[29]S. Yu, B. Huang, Q. Zeng, A. R. Oganov, L. Zhang, and G. Frapper, "Emergence of novel polynitrogen molecule-like species, covalent chains, and layers in magnesium–mitrogen Mg_xN_y under high pressure," J. Phys. Chem. C **121**, 11037–11046 (2017).
[30]S. Zhang, Z. Zhao, L. Liu, and G. Yang, "Pressure-induced stable BeN_4 as a high-energy density material," J. Power Sources **365**, 155–161 (2017).
[31]L. Wu, R. Tian, B. Wan, H. Liu, N. Gong, P. Chen, T. Shen, Y. Yao, H. Gou, and F. Gao, "Prediction of stable iron nitrides at ambient and high pressures with progressive formation of new polynitrogen species," Chem. Mater. **30**, 8476–8485 (2018).
[32]X.-H. Shi, B. Liu, Z. Yao, and B.-B. Liu, "Pressure-stabilized new phase of CaN_4," Chin. Phys. Lett. **37**, 047101 (2020).
[33]S. Niu, Z. Li, H. Li, X. Shi, Z. Yao, and B. Liu, "New cadmium–nitrogen compounds at high pressures," Inorg. Chem. **60**, 6772–6781 (2021).
[34]M. Bykov, E. Bykova, G. Aprilis, K. Glazyrin, E. Koemets, I. Chuvashova, I. Kupenko, C. McCammon, M. Mezouar, V. Prakapenka, H. P. Liermann, F. Tasnádi, A. V. Ponomareva, I. A. Abrikosov, N. Dubrovinskaia, and L. Dubrovinsky, "Fe-N system at high pressure reveals a compound featuring polymeric nitrogen chains," Nat. Commun. **9**, 2756 (2018).
[35]D. Laniel, B. Winkler, E. Koemets, T. Fedotenko, M. Bykov, E. Bykova, L. Dubrovinsky, and N. Dubrovinskaia, "Synthesis of magnesium-nitrogen salts of polynitrogen anions," Nat. Commun. **10**, 4515 (2019).
[36]M. Bykov, T. Fedotenko, S. Chariton, D. Laniel, K. Glazyrin, M. Hanfland, J. S. Smith, V. B. Prakapenka, M. F. Mahmood, A. F. Goncharov, A. V. Ponomareva, F. Tasnádi, A. I. Abrikosov, T. Bin Masood, I. Hotz, A. N. Rudenko, M. I. Katsnelson, N. Dubrovinskaia, L. Dubrovinsky, and I. A. Abrikosov, "High-pressure synthesis of Dirac materials: Layered van der Waals bonded BeN_4 polymorph," Phys. Rev. Lett. **126**, 175501 (2021).
[37]M. Bykov, E. Bykova, A. V. Ponomareva, I. A. Abrikosov, S. Chariton, V. B. Prakapenka, M. F. Mahmood, L. Dubrovinsky, and A. F. Goncharov, "Stabilization of polynitrogen anions in tantalum–nitrogen compounds at high pressure," Angew. Chem., Int. Ed. **60**, 9003–9008 (2021).
[38]M. Bykov, E. Bykova, E. Koemets, T. Fedotenko, G. Aprilis, K. Glazyrin, H.-P. Liermann, A. V. Ponomareva, J. Tidholm, F. Tasnádi, I. A. Abrikosov, N. Dubrovinskaia, and L. Dubrovinsky, "High-pressure synthesis of a nitrogen-rich inclusion compound $ReN_8{\cdot}xN_2$ with conjugated polymeric nitrogen chains," Angew. Chem., Int. Ed. **57**, 9048–9053 (2018).
[39]M. Bykov, S. Chariton, E. Bykova, S. Khandarkhaeva, T. Fedotenko, A. V. Ponomareva, J. Tidholm, F. Tasnádi, I. A. Abrikosov, P. Sedmak, V. Prakapenka, M. Hanfland, H. P. Liermann, M. Mahmood, A. F. Goncharov, N. Dubrovinskaia, and L. Dubrovinsky, "High-pressure synthesis of metal–inorganic frameworks $Hf_4N_{20}{\cdot}N_2$, $WN_8{\cdot}N_2$, and $Os_5N_{28}{\cdot}3N_2$ with polymeric nitrogen linkers," Angew. Chem., Int. Ed. **59**, 10321–10326 (2020).
[40]K. Xia, H. Gao, C. Liu, J. Yuan, J. Sun, H.-T. Wang, and D. Xing, "A novel superhard tungsten nitride predicted by machine-learning accelerated crystal structure search," Sci. Bull. **63**, 817–824 (2018).
[41]H. Gao, J. Wang, Y. Han, and J. Sun, "Enhancing crystal structure prediction by decomposition and evolution schemes based on graph theory," Fundam. Res. **1**, 466–471 (2021).
[42]H. Gao, J. Wang, Z. Guo, and J. Sun, "Determining dimensionalities and multiplicities of crystal nets," npj Comput. Mater. **6**, 143 (2020).
[43]C. Liu, H. Gao, Y. Wang, R. J. Needs, C. J. Pickard, J. Sun, H.-T. Wang, and D. Xing, "Multiple superionic states in helium–water compounds," Nat. Phys. **15**, 1065–1070 (2019).
[44]Q. Gu, D. Xing, and J. Sun, "Superconducting single-layer T-graphene and novel synthesis routes," Chin. Phys. Lett. **36**, 097401 (2019).
[45]C. Liu, H. Gao, A. Hermann, Y. Wang, M. Miao, C. J. Pickard, R. J. Needs, H.-T. Wang, D. Xing, and J. Sun, "Plastic and superionic helium ammonia compounds under high pressure and high temperature," Phys. Rev. X **10**, 021007 (2020).
[46]H. Gao, C. Liu, A. Hermann, R. J. Needs, C. J. Pickard, H.-T. Wang, D. Xing, and J. Sun, "Coexistence of plastic and partially diffusive phases in a helium-methane compound," Natl. Sci. Rev. **7**, 1540–1547 (2020).
[47]C. Liu, J. Shi, H. Gao, J. Wang, Y. Han, X. Lu, H. T. Wang, D. Xing, and J. Sun, "Mixed coordination silica at megabar pressure," Phys. Rev. Lett. **126**, 035701 (2021).
[48]C. Ding, J. Wang, Y. Han, J. Yuan, H. Gao, and J. Sun, "High energy density polymeric nitrogen nanotubes inside carbon nanotubes," Chin. Phys. Lett. **39**, 036101 (2022).
[49]G. Kresse and J. Furthmüller, "Efficient iterative schemes for *ab initio* total-energy calculations using a plane-wave basis set," Phys. Rev. B **54**, 11169–11186 (1996).
[50]P. E. Blöchl, "Projector augmented-wave method," Phys. Rev. B **50**, 17953–17979 (1994).
[51]J. P. Perdew, A. Ruzsinszky, G. I. Csonka, O. A. Vydrov, G. E. Scuseria, L. A. Constantin, X. Zhou, and K. Burke, "Restoring the density-gradient expansion for exchange in solids and surfaces," Phys. Rev. Lett. **100**, 136406 (2008).
[52]G. Kresse and D. Joubert, "From ultrasoft pseudopotentials to the projector augmented-wave method," Phys. Rev. B **59**, 1758–1775 (1999).
[53]S. Grimme, J. Antony, S. Ehrlich, and H. Krieg, "A consistent and accurate *ab initio* parametrization of density functional dispersion correction (DFT-D) for the 94 elements H-Pu," J. Chem. Phys. **132**, 154104 (2010).
[54]S. Grimme, S. Ehrlich, and L. Goerigk, "Effect of the damping function in dispersion corrected density functional theory," J. Comput. Chem. **32**, 1456–1465 (2011).
[55]A. Togo and I. Tanaka, "First principles phonon calculations in materials science," Scr. Mater. **108**, 1–5 (2015).
[56]S. Maintz, V. L. Deringer, A. L. Tchougréeff, and R. Dronskowski, "Analytic projection from plane-wave and PAW wavefunctions and application to chemical-bonding analysis in solids," J. Comput. Chem. **34**, 2557–2567 (2013).
[57]S. Maintz, V. L. Deringer, A. L. Tchougréeff, and R. Dronskowski, "LOBSTER: A tool to extract chemical bonding from plane-wave based DFT," J. Comput. Chem. **37**, 1030–1035 (2016).
[58]A. Otero-de-la-Roza, M. A. Blanco, A. M. Pendás, and V. Luaña, "Critic: A new program for the topological analysis of solid-state electron densities," Comput. Phys. Commun. **180**, 157–166 (2009).
[59]A. Otero-de-la-Roza, E. R. Johnson, and V. Luaña, "Critic2: A program for real-space analysis of quantum chemical interactions in solids," Comput. Phys. Commun. **185**, 1007–1018 (2014).
[60]K. Momma and F. Izumi, "*VESTA3* for three-dimensional visualization of crystal, volumetric and morphology data," J. Appl. Crystallogr. **44**, 1272–1276 (2011).
[61]Y. Jean, F. Volatron, and J. K. Burdett, *An Introduction to Molecular Orbitals* (Oxford University Press, New York, 1993).
[62]S. Limpijumnong and W. R. L. Lambrecht, "Homogeneous strain deformation path for the wurtzite to rocksalt high-pressure phase transition in GaN," Phys. Rev. Lett. **86**, 91–94 (2001).
[63]S. Zerroug, F. Ali Sahraoui, and N. Bouarissa, "Ab initio calculations of yttrium nitride: Structural and electronic properties," Appl. Phys. A **97**, 345–350 (2009).
[64]Z. Liu, D. Li, S. Wei, W. Wang, F. Tian, K. Bao, D. Duan, H. Yu, B. Liu, and T. Cui, "Bonding properties of aluminum nitride at high pressure," Inorg. Chem. **56**, 7494–7500 (2017).
[65]C. J. Pickard and R. J. Needs, "High-pressure phases of nitrogen," Phys. Rev. Lett. **102**, 125702 (2009).
[66]R. Y. Rohling, I. C. Tranca, E. J. M. Hensen, and E. A. Pidko, "Correlations between density-based bond orders and orbital-based bond energies for chemical bonding analysis," J. Phys. Chem. C **123**, 2843–2854 (2019).
[67]E. R. Johnson, S. Keinan, P. Mori-Sánchez, J. Contreras-García, A. J. Cohen, and W. Yang, "Revealing noncovalent interactions," J. Am. Chem. Soc. **132**, 6498–6506 (2010).
[68]W. Humphrey, A. Dalke, and K. Schulten, "VMD: Visual molecular dynamics," J. Mol. Graphics **14**, 33–38 (1996).
[69]M. J. Kamlet and S. J. Jacobs, "Chemistry of detonations. I. A simple method for calculating detonation properties of C–H–N–O explosives," J. Chem. Phys. **48**, 23–35 (1968).
[70]J. Zhang, A. R. Oganov, X. Li, and H. Niu, "Pressure-stabilized hafnium nitrides and their properties," Phys. Rev. B **95**, 020103 (2017).